Title

Dynamic MRI of the wrist in less than 20 seconds: normal midcarpal motion and reader reliability

Journal

Skeletal Radiology, 49(2)

ISSN

0364-2348

Authors

Henrichon, Stephen S
Foster, Brent H
Shaw, Calvin
et al.

Publication Date

2020-02-01

DOI

10.1007/s00256-019-03266-1

Peer reviewed

HHS Public Access

Author manuscript

Skeletal Radiol. Author manuscript; available in PMC 2021 February 01.

Published in final edited form as:

Skeletal Radiol. 2020 February ; 49(2): 241–248. doi:10.1007/s00256-019-03266-1.

Dynamic MRI of the Wrist in Less than 20 Seconds: Normal Midcarpal Motion and Reader Reliability

Stephen S. Henrichon, MD[*],
Department of Radiology, University of California - Davis, Sacramento, CA 95817

Brent H. Foster, PhD[*],
Department of Biomedical Engineering, University of California - Davis, Davis, CA 95616

Calvin Shaw, PhD,
Department of Radiology, University of California - Davis, Sacramento, CA 95817

Christopher O. Bayne, MD,
Department of Orthopaedic Surgery, University of California - Davis, Sacramento, CA 95817

Robert M. Szabo, MD, MPH,
Department of Orthopaedic Surgery, University of California - Davis, Sacramento, CA 95817

Abhijit J. Chaudhari, PhD,
Department of Radiology, University of California - Davis, Sacramento, CA 95817

Robert D. Boutin, MD
Department of Radiology, University of California - Davis, Sacramento, CA 95817

Abstract

OBJECTIVE—To describe the normal motion pattern at the midcarpal compartment during active radial-ulnar deviation of the wrist using dynamic MRI and to determine the observer performance for measurements obtained in asymptomatic volunteers.

METHODS—Dynamic MRI of 35 wrists in 19 asymptomatic volunteers (age mean 30.4 yrs, sd 8.6) was performed during active radial-ulnar deviation using a fast gradient-echo pulse sequence with 315 ms temporal resolution (acquisition time, 19 sec). Two independent readers measured the transverse translation of the trapezium at the scaphotrapezium joint (STJ) and the capitate-to-

CORRESPONDING AUTHOR: Robert D. Boutin (rdboutin@ucdavis.edu), 4860 Y Street, Suite 3100, Sacramento, CA 95817, USA Tel: 916-734-5309.
[*]Both authors contributed equally to this work.

CONFLICTS OF INTEREST: The authors declare no potential conflicts of interest with respect to the research, authorship, and/or publication of this article.

Compliance with ethical standards

All procedures performed in studies involving human participants were in accordance with the ethical standards of the institutional and/or national research committee and with the 1964 Helsinki Declaration and its later amendments or comparable ethical standards.

Based on a presentation at the RSNA 2018 annual meeting, Chicago, IL.

triquetrum distance (CTD). Relationships between these measurements and laterality, sex, lunate type, and wrist kinematic pattern were evaluated.

RESULTS—At the STJ, the trapezium moved most in radial deviation, with an overall translation of 2.3mm between ulnar and radial deviation. Mean CTD measurements were the greatest in ulnar deviation and varied 2.4mm between ulnar and radial deviation. Mean CTD was greater in men than women in the neutral position (p=0.019), as well as in wrists with type II lunate morphology during radial and ulnar deviation (p=0.001, p=0.014). There were no significant differences in trapezium translation or CTD with wrist laterality and kinematic pattern. Intraobserver and interobserver correlation coefficients were 0.97 and 0.87 for trapezium translation and 0.84 and 0.67 for CTD.

CONCLUSION—This study is the first to demonstrate the performance of dynamic MRI to quantify STJ motion and CTD. Dynamic MRI with a short acquisition time may be used as a tool to supplement static MRI in evaluation of the midcarpal compartment.

Keywords

carpal instability; dynamic; magnetic resonance imaging; radioulnar deviation; wrist

INTRODUCTION

> “Midcarpal instability…if there is one area of wrist instability that causes more confusion than any other, this is it.”
>
> - Rory Wetherell (Editor), The Journal of Hand Surgery (European Volume) [1]

Midcarpal instability is defined as a functional instability that occurs between the proximal and distal carpal rows [2]. Patients with midcarpal instability most often present with poorly localized wrist pain and dysfunction, and may have a history of trauma or ligamentous laxity [3]. On physical examination, symptoms may be reproduced while stressing the midcarpal articulation, classically with abnormal mobility, an unpredictable “blockade” feeling, or an observable “clunk” [4]. Clinical diagnosis can be difficult, causative pathomechanics are poorly understood, and optimal management remains controversial [5–7]. Currently, non-operative and operative treatments are guided generally by the type and grade of midcarpal instability assessed clinically [8]. Although kinematics involving the scaphotrapezium joint (STJ) has been studied with CT in a small number of cadavers [9] and healthy subjects [10], little is known about normal motion patterns *in vivo* using MRI. Analysis of the transverse translation of the trapezium may be useful for characterizing *in vivo* kinematics at the STJ [9], which is the second most common site for osteoarthritis in the wrist.

Midcarpal motion patterns may be affected by dynamic and anatomic factors. With respect to *dynamic* factors, “row” and “column” kinematic patterns may be implicated in understanding midcarpal instability [11]. In brief, with relatively rigid “row” wrists, the scaphoid exhibits minimal flexionextension during radial-ulnar deviation, whereas with relatively lax “column” wrists, there is a dominant pattern of scaphoid flexion-extension out of the coronal plane during the same maneuver. With respect to *anatomic* factors, lunate morphology may play an important role in influencing midcarpal motion patterns [12, 13]

(Table 1). Specifically, in lunates with a facet that articulates with the hamate, referred to as type II lunates [14], there is an association with a wider capitate-to-triquetrum distance (CTD) in the midcarpal compartment and with full-thickness perforation of the lunotriquetral ligament in patients with pain assessed by MR arthrography [15] and arthroscopy [16].

Diagnostic imaging of dynamic wrist instability may include radiography [17], cineradiography [18], fluoroscopy [19], sonography [20], and CT [21–23]. Although MRI exams are generally performed in the neutral position with a static technique, fast MRI has been used during active motion ("dynamic MRI") to evaluate kinematics of the proximal carpal row, the distal radioulnar joint, and the extensor carpi ulnaris tendon [24, 25]. Dynamic MRI, in comparison to dynamic CT, has potential advantages, including the lack of ionizing radiation and the ability to acquire images quickly as a supplement to routine MRI exams. Early results of dynamic MRI in the musculoskeletal system are encouraging for evaluating functional anatomy and pain mechanisms, but they must be evaluated with caution until fundamental performance measures such as metrological reliability are determined [26]. To our knowledge, dynamic MRI has not been used to evaluate midcarpal motion patterns or the reliability of MRI-derived metrics.

The purpose of this study was to use dynamic MRI of the wrist in asymptomatic volunteers to (1) examine midcarpal motion patterns at the STJ and the CTD during the uninterrupted radial and ulnar deviation maneuvers and (2) determine the observer performance of measurements in asymptomatic volunteers.

MATERIALS AND METHODS

Subjects

This prospective study received approval by our institutional review board. Participants responded to flyers with study information posted at our medical center. Written informed consent was obtained from all individual participants included in the study. The study cohort consisted of 20 consecutive volunteers recruited at our university between February 2017 and November 2017. (No prospective sample size calculation was performed given the pilot nature of the study, as there were no prior data to use for such a calculation.) Inclusion criteria were healthy, asymptomatic subjects between the ages of 18 and 55 years without a history of wrist trauma, wrist pain, or prior wrist surgery. Subjects were excluded if they had a contraindication to MRI (n=0) or could not complete a wrist MRI examination (n=1). The remaining 19 subjects, 10 men and 9 women, had a mean age of 30.4 ± 8.6 years (range 20–55). The ethnicity of recruited participants was as follows: White (N=14), Asian (N=6), and Hispanic or Latino (N=1). Eighteen volunteers had both wrists scanned while 1 volunteer had only the right wrist scanned (due to discomfort during scanning) for a total of 37 wrist scans. Two scans were excluded due to participant non-compliance during performance of the maneuver, yielding a total of 35 wrist MRI examinations for evaluation.

MRI Protocol

Images were acquired with a 3.0-T MRI scanner (Skyra, Siemens Healthcare, Erlangen, Germany), with volunteers in a head-first, prone ("superman") position. The volunteers moved their wrist in a continuous radial-ulnar deviation motion during the acquisition, achieving maximum range of motion. The dynamic MRI pulse sequence used was a multi-slice 2D radially acquired fast-gradient echo sequence with water excitation, known by the vendor as fast low angle shot (FLASH) (field-of-view = 120 mm^2, matrix size = 112 × 112, number of radial spokes = 100, TR/TE =3.15/1.74 ms, bandwidth = 990 Hz/pixel, flip angle = 12 deg). The reconstructed voxel size was 1.07 × 1.07 mm, with a slice thickness of 6 mm and a temporal resolution of 315 ms per 2D slice. Ten time points were sequentially acquired with six 2D slices per time point. The total acquisition time was 18.9 sec. This acquisition scheme was chosen to complement the typical musculoskeletal MRI exam that optimizes for spatial and contrast resolution; the dynamic images were optimized for temporal resolution, while attempting to retain adequate contrast for the carpal bones, signal-to-noise ratio, and slice thickness [24]. A representative sample of images using this technique is displayed in Fig. 1.

Measurements

From the dynamic MRI scans, representative images showing the STJ and CTD were identified and used for quantification by two independent readers (a fellow in musculoskeletal radiology and a PhD in biomedical engineering). Both readers were trained by a senior musculoskeletal radiologist with 22 years of post-training experience and their performance was evaluated on a separate dataset by the senior radiologist to ensure adequacy of training. Then, each reader measured the translation of the trapezium with respect to the scaphoid with the wrist in neutral, as well as maximal ulnar deviation and maximal radial deviation, using the open-source ImageJ image analysis software (National Institutes of Health, Bethesda, Maryland, https://imagej.nih.gov/ij/). Specifically, translation was evaluated by first drawing a line parallel to the distal articular surface of the scaphoid, then drawing a second line perpendicular to the distal articular surface of the scaphoid along the radial edge of the articular surface, and lastly measuring the translation of the trapezium from this perpendicular line. Fig. 2 provides a schematic of the anatomic landmarks used for measurements. Fig. 3 shows the location of representative measurements of dynamically acquired images. (A positive value was recorded for translation of the trapezium in the radial direction, whereas a negative value was recorded for translation in the ulnar direction.) Similarly, CTD was evaluated on images with the wrist in neutral, in maximum radial deviation, and in maximum ulnar deviation. As described by previous investigators [15], the CTD was measured from the radial aspect of the triquetrum to the ulnar aspect of the capitate. For determination of row versus column kinematic patterns on MRI, we modified the methods described by Garcia-Elias et al [27] that evaluated scaphoid flexion during radial and ulnar deviation on frontal radiographs. In this method, the kinematic pattern was determined in a binary fashion by reader consensus based on flexion/extension of the scaphoid (minimal = row; moderate = column) using multislice coronal MR images at maximal radial and ulnar deviation.

After 2 weeks from the time of the initial measurements, repeat measurements were performed by the first reader on all scans to assess intraobserver reliability.

Statistical Analysis

A two-sample Kolmogorov-Smirnov goodness-of-fit hypothesis test was performed to test statistical significance differences in the imaging measures between lunate type (type I vs. II), wrist type (row vs. column), sex (male vs. female), and side (left vs. right). The intraclass correlation coefficient (ICC) was computed to quantify intraobserver and interobserver reliability for the imaging measures performed. The following grading scale was used for the ICC: poor (<0.40), fair (0.40 – 0.59), good (0.60 – 0.74), and excellent (0.75 – 1.00) [28]. In each case, statistical significance was assigned based on $p < 0.05$.

RESULTS

Measurements made at the STJ and the CTD during dynamic MRI are detailed in Table 2. The trapezium moved most in radial deviation, with an overall mean translation of 2.3 mm between ulnar and radial deviation. The CTD was greatest in ulnar deviation, with a mean change of 2.4 mm from radial deviation.

Trapezium translation and CTD mean measurements with respect to wrist laterality, sex, lunate type, and wrist kinematic pattern are also shown in Table 3. There were no significant differences in either metric when comparing the left wrists versus the right wrists in our cohort. When comparing differences in these metrics by sex, men had an overall greater CTD than women, although results were only significant in the neutral position (p=0.019). The CTD was larger in wrists with type II lunates compared to type I lunates during radial deviation (p=0.001) and ulnar deviation (p=0.014). When comparing row versus column wrist kinematic patterns, there were no statistically significant differences in the two metrics.

The trapezium translation had an intraobserver ICC of 0.97 (95% CI=0.93–0.99) and an interobserver ICC of 0.87 (95% CI=0.69–0.95). The CTD had an intraobserver ICC of 0.84 (95% CI=0.62–0.94) and an interobserver ICC of 0.67 (95% CI=0.29–0.87).

DISCUSSION

Our study found that the trapezium normally translates transversely relative to the scaphoid, and this translation occurs asymmetrically more in radial deviation than ulnar deviation. These findings complement prior research by Moritomo et al [9] on the scaphotrapezium-trapezoid joint that found an oblique-sagittal rotational motion occurs at the scaphotrapezoid joint during radial and ulnar deviation of the wrist, but that the trapezium-trapezoid joint remained essentially immobile during this maneuver. Our findings are consistent with Sonenblum et al [10] who examined ten healthy volunteers by CT and found that there is movement of the trapezium and trapezoid relative to the scaphoid in ulnar deviation. We are not aware of prior published work that specifically evaluates trapezium translation with respect to the scaphoid at the STJ by MRI.

In our population of asymptomatic volunteers, we found no difference in trapezium translation with wrist laterality, sex, lunate type, or wrist kinematic pattern. Although there is one case report of wrist motion studied with a scaphoid-trapezium coalition [29], it remains unclear how the trapezium moves in patients with other pathologic conditions, such as STJ osteoarthritis or collagen disorders (associated with ligamentous laxity), which is a consideration for future research. The scaphotrapezium-trapezoid joint is the second most common site for osteoarthritis in the wrist and has a well-known association with the most common site for osteoarthritis in the upper extremity: the first carpometacarpal joint. It is less well known that osteoarthritis at the scaphotrapezium-trapezoid joint can cause decreased thumb range of motion and grip strength [30], and that it is associated with type II lunate morphology [31], a widened scapholunate gap (> 3 mm) [32], and DISI-like midcarpal instability [33]. This midcarpal instability may worsen after surgical intervention (e.g., open or arthroscopic resection arthroplasty), while pre-operative diagnosis of instability could reduce the number of unsatisfied patients [34]. Dorsal intercalated segment instability (DISI) represents a carpal instability pattern in which there is compromise of the radial ligamentous structures of the wrist, resulting in dorsal rotation of the lunate. While several injuries may result in lunate dorsal rotation, DISI is most characteristically associated with injury to scapholunate ligament and supporting ligamentous structures. This injury allows the scaphoid to flex and the lunate and triquetrum to extend, causing a widened scapholunate interval on posteroanterior radiographs and an increased scapholunate angle on lateral radiographs. While distinct from classic DISI deformity, lunate dorsal extension can also be caused by scaphotrapezium-trapezoid joint arthritis. In this condition, arthritis decreases motion at the scaphotrapezium-trapezoid joint, locking the scaphoid in a relative position of extension. The lunate is forced into extension by the extended scaphoid through an intact scapholunate ligament.

We found the CTD to be wider in wrists with type II lunates, which is consistent with prior research [15, 35]. We also observed that the CTD was wider in male wrists in the neutral position only, which is also in line with prior research [15]. The CTD has been found to be clinically relevant in the setting of many common wrist derangements. In the setting of static scapholunate instability, carpal collapse is reportedly less likely in patients with an increased CTD (≥ 5 mm) [36]. Type II lunate morphology and wider CTD also have been associated with decreased DISI deformity and more proximally located fractures in patients presenting with scaphoid nonunion [35]. Finally, an increased CTD has been associated with ulnar impaction syndrome [37] and full-thickness lunotriquetral ligament tears [15].

When comparing row versus column wrist kinematic patterns, we found no difference in trapezium translation and CTD. To our knowledge, there are no prior reports of row and column kinematic analysis using dynamic MRI. Knowledge of the normal motion pattern at the midcarpal compartment during active radial and ulnar deviation of the wrist could potentially be useful in understanding and diagnosing dynamic features of midcarpal instability, as well as treatments of various scapholunate instability patterns (e.g., scaphotrapezium-trapezoid fusion) [38–39]. For example, patients with pre-dynamic instability currently represent a diagnostic challenge. They present with normal stress and non-stress radiographs. However, these patients may demonstrate ligamentous pathology on MRI or during arthroscopy. Unfortunately, ligamentous derangements as diagnosed by MRI

or arthroscopy may be incidental, and patients with these findings do not always suffer from altered carpal mechanics. Dynamic MRI has the potential to successfully evaluate symptomatic patients by simultaneously diagnosing ligamentous pathology and evaluating carpal motion.

Our study should be accessed in the context of limitations that could be addressed with future research. First, we studied a relatively small cohort of 35 wrists in 19 asymptomatic volunteers. However, this cohort size is in line with prior literature evaluating clinical [5, 8, 40–42], biomechanical [6, 43–45], and dynamic CT [21–23, 46–49] aspects of wrist disorders. Although our analysis serves as a foundation for future work on normal and abnormal kinematic patterns, we did not analyze symptomatic patients or have clinical justification to correlate findings with radiography, fluoroscopy, CT, or histopathology in our asymptomatic volunteers. Second, because the high *temporal resolution* (315 ms) resulted in diminished in-plane spatial resolution compared to routine clinical scans, we emphasize that dynamic imaging should be employed as a supplement to conventional static MRI protocols that use a high *spatial resolution* technique. That said, the intriguing possibility is that fast (e.g., 20 sec) acquisitions with high temporal resolution techniques might complement conventional MRI. Current work in this area leverages the high spatial resolution static image data for the purpose of autosegmentation of carpal bones in motion during real-time wrist MRI exams [50]. Third, in this study, 2D multi-slice scans were acquired only in the coronal plane. However, wrist kinematics and pathomechanics are complex phenomena that occur in three dimensions, and there is considerable interest in studying midcarpal motion and instability that also occurs in the sagittal plane [4–8, 40–42]. Advances in MRI technology are expected to enable implementation of true “4D” acquisitions that combine 3D volumetric datasets with the added dimension of time. Finally, there may be differences between radiographic and cross-sectional techniques for assessment of wrist kinematics, but we are not aware of prior research using dynamic MRI to analyze row and column patterns.

In conclusion, our study provides a preliminary evaluation of midcarpal motion patterns, specifically involving the STJ and CTD, in asymptomatic wrists. Dynamic MRI can be acquired on conventional MRI scanners and has excellent intraobserver and interobserver reliability. It could become a promising tool to supplement high spatial resolution static scans by using real-time images with short acquisition times.

Supplementary Material

Refer to Web version on PubMed Central for supplementary material.

Acknowledgements

The authors gratefully acknowledge the assistance of John Brock in assisting with IRB compliance, Julie Ostoich-Prather in assisting with graphic design, as well as Gerald Sonico, B.S., Costin Tanase, PhD, and Sinyeob Ahn, PhD in assisting with optimizing real-time pulse sequence parameters.

Grant support

National Institutes of Health (K12 HD051958 and R03 EB015099) to Abhijit J. Chaudhari, and National Science Foundation (GRFP Grant No. 1650042) to Brent Foster.

REFERENCES

1. Wetherell R Special issue: the unstable wrist. J Hand Surg Eur Vol. 2016;41(1):5–6. [PubMed: 26685201]
2. Hargreaves DG. Midcarpal instability. J Hand Surg Eur Vol. 2016;41(1):86–93. [PubMed: 26598109]
3. Lichtman DM, Wroten ES. Understanding midcarpal instability. J Hand Surg Am. 2006;31(3):491–498. [PubMed: 16516747]
4. Mulders MAM, Sulkers GSI, Videler AJ, Strackee SD, Smeulders MJC. Long-term functional results of a wrist exercise program for patients with palmar midcarpal instability. J Wrist Su irg. 2018;7(3):211–218.
5. Ho PC, Tse WL, Wong CW. Palmar midcarpal instability: an algorithm of diagnosis and surgical management. J Wrist Surg. 2017;6(4): 262–275. [PubMed: 29085727]
6. Shiga SA, Werner FW, Garcia-Elias M, Harley BJ. Biomechanical analysis of palmar midcarpal instability and treatment by partial wrist arthrodesis. J Hand Surg Am. 2018;43(4):331–338.e2. [PubMed: 29146508]
7. Niacaris T, Ming BW, Lichtman DM. Midcarpal instability: a comprehensive review and update. Hand Clin. 2015;31(3):487–493. [PubMed: 26205710]
8. Higgin RPC, Hargreaves DG. Midcarpal instability: the role of wrist arthroscopy. Hand Clin. 2017;33(4):717–726. [PubMed: 28991583]
9. Moritomo H, Viegas SF, Elder K, Nakamura K, Dasilva MF, Patterson RM. The scaphotrapezio-trapezoidal joint. Part 2: A kinematic study. J Hand Surg Am. 2000;25(5):911–920. [PubMed: 11040306]
10. Sonenblum SE, Crisco JJ, Kang L, Akelman E. In vivo motion of the scaphotrapezio-trapezoidal (STT) joint. J Biomech. 2004;37(5):645–652. [PubMed: 15046993]
11. Rainbow MJ, Wolff AL, Crisco JJ, Wolfe SW. Functional kinematics of the wrist. J Hand Surg Eur Vol. 2016;41(1):7–21. [PubMed: 26568538]
12. McLean JM, Bain GI, Watts AC, Mooney LT, Turner PC, Moss M. Imaging recognition of morphological variants at the midcarpal joint. J Hand Surg Am. 2009;34(6):1044–1055. [PubMed: 19497684]
13. Nakamura K, Beppu M, Patterson RM, Hanson CA, Hume PJ, Viegas SF. Motion analysis in two dimensions of radial-ulnar deviation of type I versus type II lunates. J Hand Surg Am. 2000;25(5): 877–888. [PubMed: 11040303]
14. Malik AM, Schweitzer ME, Culp RW, Osterman LA, Manton G. MR imaging of the type II lunate bone: frequency, extent, and associated findings. AJR Am J Roentgenol. 1999;173(2):335–338. [PubMed: 10430130]
15. Borgese M, Boutin RD, Bayne CO, Szabo RM, Chaudhari AJ. Association of lunate morphology, sex, and lunotriquetral interosseous ligament injury with radiologic measurement of the capitate-triquetrum joint. Skeletal Radiol. 2017;46(12):1729–1737. [PubMed: 28828602]
16. Harley BJ, Werner FW, Boles SD, Palmer AK. Arthroscopic resection of arthrosis of the proximal hamate: a clinical and biomechanical study. J Hand Surg Am. 2004;29(4):661–667. [PubMed: 15249091]
17. Lee SK, Desai H, Silver B, Dhaliwal G, Paksima N. Comparison of radiographic stress views for scapholunate dynamic instability in a cadaver model. J Hand Surg Am. 2011;36(7):1149–n57. [PubMed: 21676555]
18. Sulkers GS, Strackee SD, Schep NW, Maas M. Wrist cineradiography: a protocol for diagnosing carpal instability. Journal of Hand Surgery (European Volume). 2018;43(2):174–8.
19. Braunstein EM, Louis DS, Greene TL, Hankin FM. Fluoroscopic and arthrographic evaluation of carpal instability. AJR Am J Roentgenol. 1985;144(6):1259–1262. [PubMed: 3873808]
20. Gondim Teixeira PA, Badr S, Hossu G, et al. Quantitative analysis of scapholunate diastasis using stress speckle-tracking sonography: a proof-of-concept and feasibility study. Eur Radiol. 2017;27(12):5344–5351. [PubMed: 28656466]

21. Abou Arab W, Rauch A, Chawki MB, et al. Scapholunate instability: improved detection with semiautomated kinematic CT analysis during stress maneuvers. Eur Radiol. 2018;28(10):4397–4406. [PubMed: 29713765]
22. Mat Jais IS, Tay SC. Kinematic analysis of the scaphoid using gated four-dimensional CT. Clin Radiol. 2017;72(9):794.e1–794.e9.
23. Demehri S, Hafezi-Nejad N, Morelli JN, et al. Scapholunate kinematics of asymptomatic wrists in comparison with symptomatic contralateral wrists using four-dimensional CT examinations: initial clinical experience. Skeletal Radiol. 2016;45(4):437–446. [PubMed: 26659662]
24. Boutin RD, Buonocore MH, Immerman I, Ashwell Z, Sonico GJ, Szabo RM, Chaudhari AJ. Realtime magnetic resonance imaging (MRI) during active wrist motion-initial observations. PLoS One. 2013;31;8(12):e84004. [PubMed: 24391865]
25. Langner I, Fischer S, Eisenschenk A, Langner S. Cine MRI: a new approach to the diagnosis of scapholunate dissociation. Skeletal Radiol. 2015;44(8):1103–1110. [PubMed: 25761726]
26. Borotikar B, Lempereur M, Lelievre M, Burdin V, Ben Salem D, Brochard S. Dynamic MRI to quantify musculoskeletal motion: A systematic review of concurrent validity and reliability, and perspectives for evaluation of musculoskeletal disorders. PLoS One. 2017 12 12;12(12):e0189587. [PubMed: 29232401]
27. Garcia-Elias M, Ribe M, Rodriguez J, Cots M, Casas J. Influence of joint laxity on scaphoid kinematics. J Hand Surg Br. 1995;20(3):379–382. [PubMed: 7561416]
28. Cicchetti DV. Guidelines, criteria, and rules of thumb for evaluating normed and standardized assessment instruments in psychology. Psychological assessment. 1994;6(4):284–290.
29. Yukioka C, Arimitsu S, Moritomo H. Three-dimensional kinematic analysis of a scaphoid-trapezium coalition: A case report. J Hand Surg Eur Vol. 2016;41(5):554–555. [PubMed: 25311935]
30. Pegoli L, Pozzi A, Pivato G, Luchetti R. Arthroscopic resection of distal pole of the scaphoid for scaphotrapeziotrapezoid joint arthritis: comparison between simple resection and implant interposition. J Wrist Surg. 2016;5(3):227–232. [PubMed: 27468374]
31. McLean JM, Turner PC, Bain GI, Rezaian N, Field J, Fogg Q. An association between lunate morphology and scaphoid-trapezium-trapezoid arthritis. J Hand Surg Eur Vol. 2009;34(6):778–782. [PubMed: 19786403]
32. Scordino LE, Bernstein J, Nakashian M, et al. Radiographic prevalence of scaphotrapeziotrapezoid osteoarthrosis. J Hand Surg Am. 2014;39(9):1677–1682. [PubMed: 25037508]
33. Tay SC, Moran SL, Shin AY, Linscheid RL. The clinical implications of scaphotrapezium-trapezoidal arthritis with associated carpal instability. J Hand Surg Am. 2007;32(1):47–54. [PubMed: 17218175]
34. Kapoutsis DV, Dardas A, Day CS. Carpometacarpal and scaphotrapeziotrapezoid arthritis: arthroscopy, arthroplasty, and arthrodesis. J Hand Surg Am. 2011;36(2):354–366. [PubMed: 21276902]
35. Kim BJ, Kovacevic D, Lee YM, Seol JH, Kim MS. The role of lunate morphology on scapholunate instability and fracture location in patients treated for scaphoid nonunion. Clin Orthop Surg. 2016;8(2):175–180. [PubMed: 27247743]
36. Dimitriadis A, Paraskevas G, Kanavaros P, Barbouti A, Vrettakos A, Kitsoulis P. Association between the capitate-triquetrum distance and carpal collapse in static scapholunate instability. Acta Orthop Belg. 2018;84(1):68–72. [PubMed: 30457502]
37. Park JH, Jang WY, Kwak DH, Park JW. Lunate morphology as a risk factor of idiopathic ulnar impaction syndrome. Bone Joint J. 2017;99-B(11):1508–1514. [PubMed: 29092991]
38. Andersson JK. Treatment of scapholunate ligament injury: Current concepts. EFORT Open Rev. 2017;2(9):382–393. [PubMed: 29071123]
39. Watson HK, Sorelle JR, Wollstein R, Hass EAL. STT Arthrodesis In: Gelberman RH, ed. Master Techniques in Orthopaedic Surgery: The Wrist. Philadelphia: Lippincott Williams & Wilkins; 2012 p. 263–270.
40. Farr S, Schachinger F, Girsch W. Palmar Capsuloligamentous Plication in Dorsal Capitolunate Instability: Technique and Preliminary Results. Tech Hand Up Extrem Surg. 2019;23(1):22–26. [PubMed: 30461571]

41. von Schroeder HP. Dorsal Wrist Plication for Midcarpal Instability. J Hand Surg Am. 2018;43(4): 354–359. [PubMed: 29241841]

42. Shunmugam M, Phadnis J, Watts A, Bain GI. Lunate fractures and associated radiocarpal and midcarpal instabilities: a systematic review. J Hand Surg Eur Vol. 2018;43(1):84–92.41. [PubMed: 29132239]

43. Kane PM, Vopat BG, Mansuripur PK, et al. Relative Contributions of the Midcarpal and Radiocarpal Joints to Dart-Thrower's Motion at the Wrist. J Hand Surg Am. 2018;43(3):234–240. [PubMed: 29146510]

44. McNary SM, Heyrani N, Volk I, Szabo RM, Bayne CO. The Effect of Radioscapholunate Fusion With and Without Distal Scaphoid and Triquetrum Excision on Capitolunate Contact Pressures. J Hand Surg Am. 2019;44(5):420.e1–420.e7. [PubMed: 30241977]

45. Dimitris C, Werner FW, Joyce DA, Harley BJ. Force in the Scapholunate Interosseous Ligament During Active Wrist Motion. J Hand Surg Am. 2015;40(8):1525–33. [PubMed: 26026356]

46. de Roo MGA, Muurling M, Dobbe JGG, Brinkhorst ME, Streekstra GJ, Strackee SD. A four-dimensional-CT study of in vivo scapholunate rotation axes: possible implications for scapholunate ligament reconstruction. J Hand Surg Eur Vol. 2019;44(5):479–487. [PubMed: 30813846]

47. Kelly PM, Hopkins JG, Furey AJ, Squire DS. Dynamic CT Scan of the Normal Scapholunate Joint in a Clenched Fist and Radial and Ulnar Deviation. Hand (N Y). 2018;13(6):666–670. [PubMed: 28850255]

48. Kakar S, Breighner RE, Leng S, et al. The Role of Dynamic (4D) CT in the Detection of Scapholunate Ligament Injury. J Wrist Surg. 2016;5(4):306–310. [PubMed: 27777822]

49. Carr R, MacLean S, Slavotinek J, Bain GI. Four-Dimensional Computed Tomography Scanning for Dynamic Wrist Disorders: Prospective Analysis and Recommendations for Clinical Utility. J Wrist Surg. 2019;8(2):161–167. [PubMed: 30941259]

50. Foster BH, Shaw CB, Boutin RD, et al. A principal component analysis-based framework for statistical modeling of bone displacement during wrist maneuvers. J Biomech. 2019;85:173–181. [PubMed: 30738587]

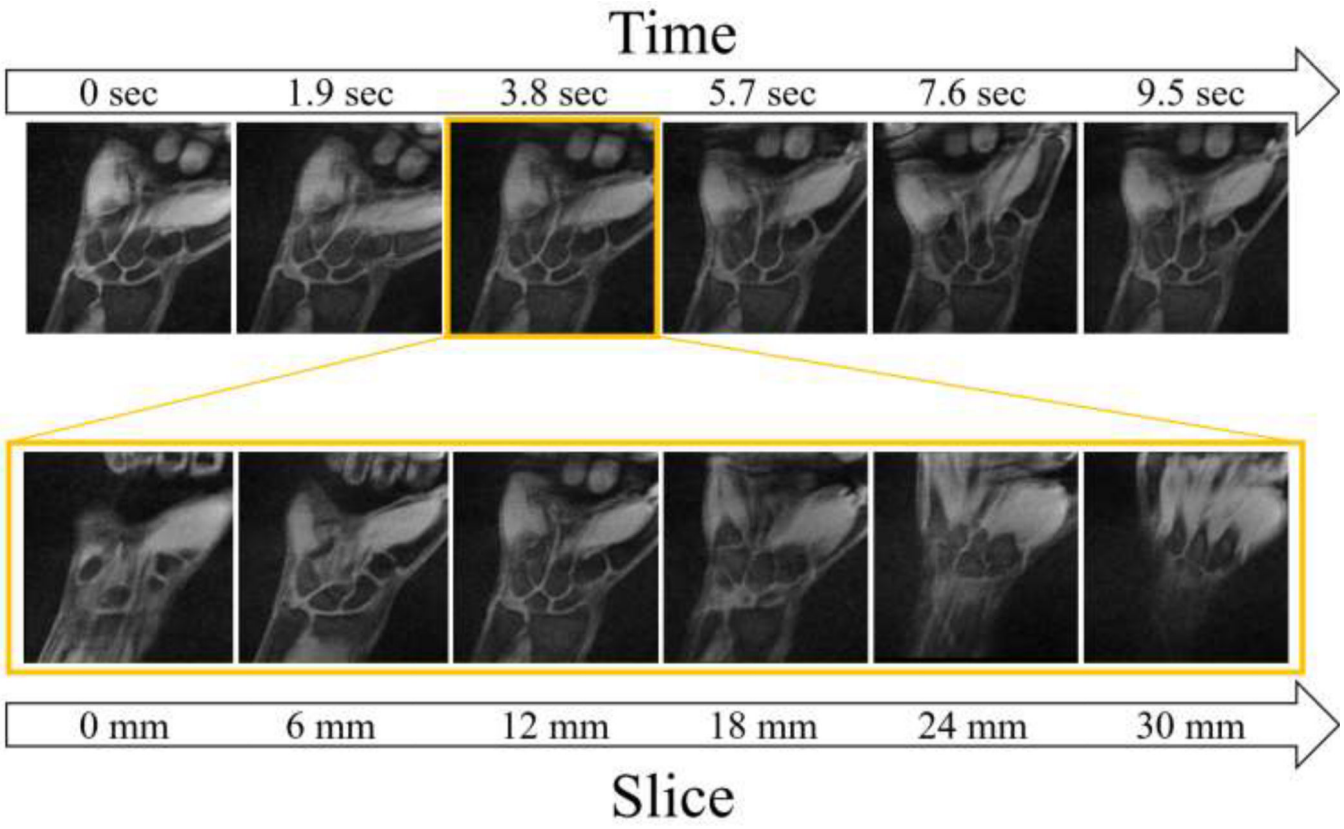

Figure 1.

27-year-old man with no history of wrist injury or pain. Representative dynamic MRI showing a 4D (3D + time) image volume of the wrist during continuous radial-ulnar deviation motion. The top row shows a single coronal slice position over time. The bottom row shows six coronal slices, which are acquired at each time point; here, at the 3.8 sec time point (from the top row).

(A)

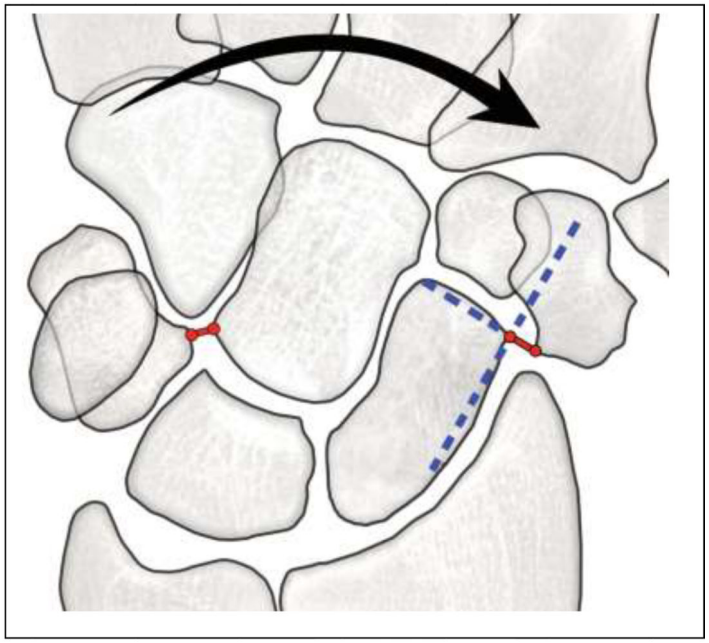

(B)

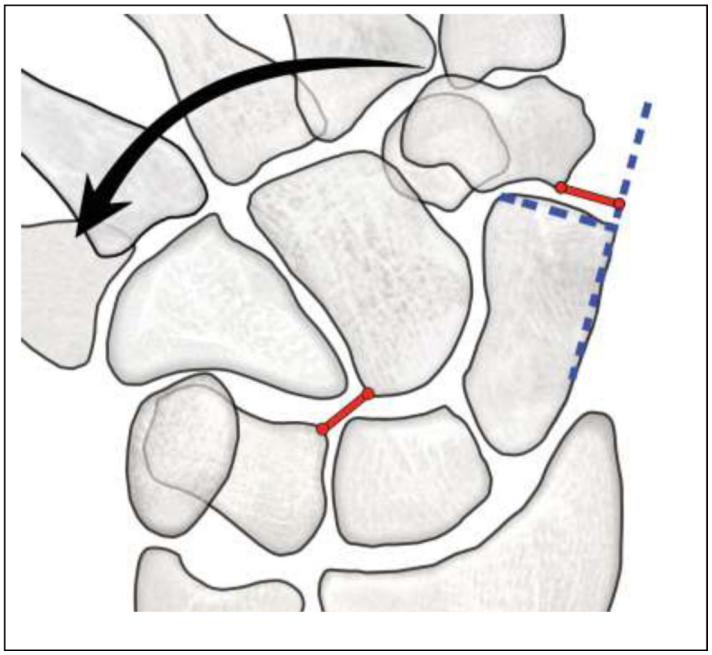

Figure 2.
Schematic of the anatomic landmarks used for measurement of trapezium translation and the capitate-triquetrum distance in radial deviation (A) and ulnar deviation (B).

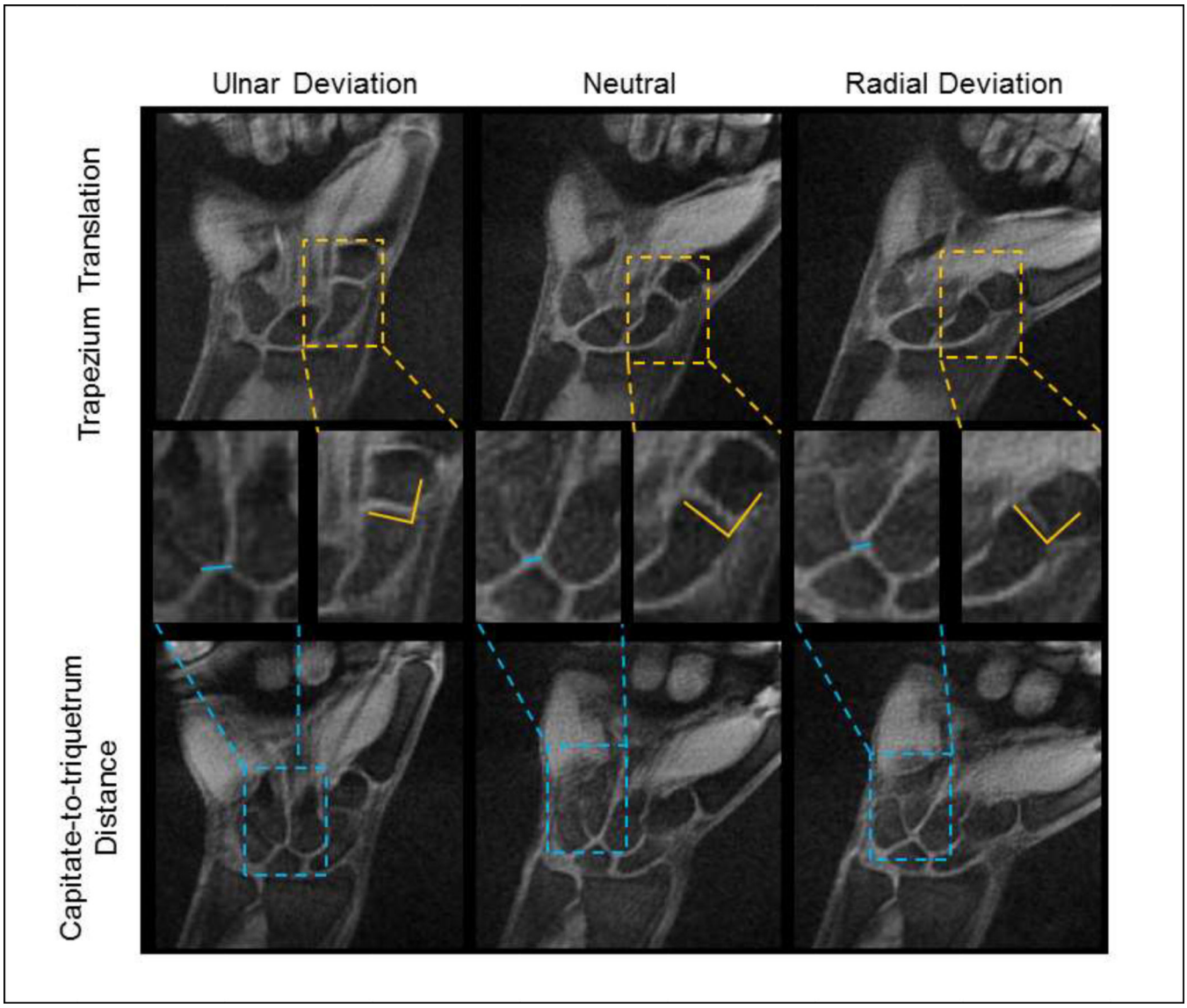

Figure 3.

27-year-old man with no history of wrist injury or pain. Coronal images from a dynamic MRI of the wrist during continuous motion. The trapezium translation (top row, orange box) and the capitate-to-triquetrum distance (bottom row, blue box) at three wrist positions: ulnar deviation, neutral, and radial deviation. Magnified inset images (middle row) show the location of representative measurements on the dynamically acquired images.

Table 1.

Lunate types analyzed

Lunate	Anatomic Features
Type I	One distal facet, articulates with the capitate No articulation with the hamate
Type II	Two distal facets (lateral and medial) Articulates with both the capitate and hamate

Table 2.

Dynamic MRI results showing midcarpal metrics of trapezium translation and capitate-to-triquetrum distance (mean +/− SD) in 35 wrists of asymptomatic volunteers.

	Trapezium Translation (mm)	Capitate-Triquetrum Distance (mm)
Neutral	0.3 +/− 0.8	5.3 +/− 1.4
Ulnar Deviation	−0.4 +/− 1.0	6.0 +/− 1.4
Radial Deviation	1.9 +/− 1.2	3.6 +/− 1.1

Table 3.

Midcarpal metrics of trapezium translation and capitate-triquetrum distance with respect to wrist laterality, sex, lunate type, and wrist kinematic pattern.

			Trapezium Translation (mm)			Capitate-Triquetrum Distance (mm)		
		Sample size (n)	**Neutral**	**Ulnar Deviation**	**Radial Deviation**	**Neutral**	**Ulnar Deviation**	**Radial Deviation**
Wrist Laterality	Left	17	0.3	−0.5	1.9	5.4	5.9	3.4
	Right	18	0.3	−0.4	2.0	5.2	6.1	3.8
	p value		0.950	1.000	0.622	1.000	0.958	0.262
Sex	Male	17	0.5	−0.2	2.1	**6.0**	6.3	3.9
	Female	18	0.1	−0.7	1.8	**4.7**	5.8	3.2
	p value		0.605	0.489	0.958	**0.019**	0.790	0.123
Lunate Type	Type I	17	0.4	−0.7	1.8	4.8	**5.4**	**2.9**
	Type II	18	0.1	−0.2	2.1	5.8	**6.6**	**4.2**
	p value		0.970	0.999	0.786	0.104	**0.014**	**0.001**
Wrist Kinematic Pattern	Row	17	0.5	−0.5	2.0	5.2	5.7	3.4
	Column	18	0.1	−0.4	1.9	5.4	6.3	3.7
	p value		0.345	0.950	0.971	1.000	0.458	0.588